



CONCN: A high-resolution, integrated surface water-groundwater ParFlow modeling platform of continental China

**Chen Yang¹, Zitong Jia², Wenjie Xu³, Zhongwang Wei¹, Xiaolang Zhang⁴, Yiguang Zou⁵,
Jeffrey McDonnell^{6,7,8}, Laura Condon⁹, Yongjiu Dai¹, Reed Maxwell¹⁰**

5 ¹School of Atmospheric Sciences, Sun Yat-sen University, Zhuhai, China

²College of Water Sciences, Beijing Normal University, Beijing, China

³Institute of Geological Survey, China University of Geosciences, Wuhan, China

⁴Department of Geosciences, Florida Atlantic University, Boca Raton, USA

⁵Department of Geography, National University of Singapore, Singapore, Singapore

10 ⁶School of Environment and Sustainability, Global Institute for Water Security, University of Saskatchewan, Saskatoon, Canada

⁷School of Geography, Earth & Environmental Sciences, University of Birmingham, Birmingham, UK.

⁸North China University of Water Resources and Electric Power, Zhengzhou 450046, China

15 ⁹Department of Hydrology and Atmospheric Sciences, University of Arizona, Tucson, USA

¹⁰Department of Civil and Environmental Engineering, Princeton University, Princeton, USA

Correspondence to: Chen Yang (yangch329@mail.sysu.edu.cn)



Abstract. Large-scale hydrologic modeling at national scale is an increasing important effort worldwide to tackle ecohydrologic issues induced by global water scarcity. In this study, a surface
25 water-groundwater integrated hydrologic modeling platform was built using ParFlow, covering the
entire continental China with a resolution of 30 arcsec. This model, CONCN 1.0, has a full
treatment of 3D variably saturated groundwater by solving Richards' equation, along with the
shallow water equation at the ground surface. The performance of CONCN 1.0 was rigorously
evaluated using both global data products and observations. RSR values show good to excellent
30 performance in streamflow, yet the streamflow is lower in the Endorheic, Hai, and Liao Rivers due
to uncertainties in potential recharge. RSR values also indicate good performance in water table
depth of the CONCN model. This is an intermediate performance compared to two global
groundwater models, highlighting the uncertainties that persist in current large-scale groundwater
modeling. Our modeling work is also a comprehensive evaluation of the current workflow for
35 continental-scale hydrologic modeling using ParFlow and could be a good starting point for the
modeling in other regions worldwide, even when using different modeling systems. More
specifically, the vast arid and semi-arid regions in China with substantial sinks (i.e., the end points
of endorheic rivers) and the large uncertainties in potential recharge pose challenges for the
numerical solution and model performance, respectively. Incompatibilities between data and
40 model, such as the mismatch of spatial resolutions between model and products and the shorter,
less frequent observation records, require further refinement of the workflow to enable fast
modeling. This work not only establishes the first integrated hydrologic modeling platform in
China for efficient water resources management, but it will also benefit the improvement of next
generation models worldwide.

45



1. Introduction

China has faced persistent water crises due to the rapid socio-economic development and population growth (Jiang, 2009), resulting in the second lowest per inhabitant water supply among all countries in the world (Pietz, 2017). The increasing water demand in China has been further
50 exacerbated by more frequent hydrologic extremes (e.g., drought and flooding) and the deterioration of water quality, caused by climate change and human activities (Wang et al., 2018). Water availability in China affects not only the trajectories of self-development but also the global food and supply chain (Collins and Reddy, 2022). Therefore, it is pressing to develop a consistent hydrologic modeling platform for China at national scale for water resources management, water
55 quality control, and decision-making. Some work has begun in this regard. A national-scale groundwater model with a 10 km resolution based on MODFLOW has been built (Lancia et al., 2022), and national-wide natural streamflow was reconstructed using the Variable Infiltration Capacity (VIC) model with a 0.25° resolution (Miao et al., 2022). Regional groundwater models or hydrologic models with a groundwater component have also been developed for many focused
60 areas, such as the North China Plain (Cao et al., 2013; Yang et al., 2020), the Heihe River Basin (Hu et al., 2016; Tian et al., 2015), the Pearl River Basin (Wang et al., 2023; Yu et al., 2022), and the Jiangnan Plain in the central Yangtze River (Jiang et al., 2022). These advances in the Chinese modeling community are valuable for quantifying fluxes, storage, and the quality of streamflow and groundwater, thereby supporting the sustainable development of China.

65 There is an increasing number of national and global modeling platforms worldwide for surface water, groundwater, or a combination of both. National-scale models include the US NOAA National Water Model (NWM) (Cosgrove et al., 2024), the USGS National Hydrologic Model (NHM) (Regan et al., 2019), the ParFlow (Parallel Flow) CONUS modeling platform (Maxwell et al., 2015; Yang et al., 2023a), the Canada National Water Model (CanadaWater) (Chen et al.,
70 2020), the British Groundwater Model (BGWM) (Bianchi et al., 2024), and the national-scale models from Germany (Belleflamme et al., 2023; Hellwig et al., 2020), France (Vergnes et al., 2023), Denmark (Henriksen et al., 2003), the Netherlands (Delsman et al., 2023), and New Zealand (Westerhoff et al., 2018). Global models include the hydrologic model WaterGap and its groundwater component G³M (Reinecke et al., 2019; Schmied et al., 2021), the hydrologic model
75 PCR-GLOBWB and its associated groundwater models (Sutanudjaja et al., 2018; Verkaik et al.,



2024; De Graaf et al., 2015; De Graaf et al., 2017; Hoch et al., 2023), and Fan's global groundwater model (Fan et al., 2013).

How to build a large-scale hydrologic model that balances high-performance with the trade-off between resolution and computational efficiency is a critical issue in the hydrologic modeling community, especially in groundwater modeling or modeling with a full treatment of groundwater. However, it remains an open question since the subsurface is largely unseen. Reinecke et al. (2020) compared the performance of several popular global groundwater models in New Zealand, along with the New Zealand national groundwater model (Westerhoff et al., 2018). Reinecke et al. (2020) attributed the departure of simulations from observations to model resolution, but Yang et al. (2023a) suggested that the model's structure and parameters also play a role. Significant progresses or consensus have been achieved in community discussions regarding model parameterization, evaluation, calibration, and intercomparison (Gleeson et al., 2021; Condon et al., 2021; O'Neill et al., 2021; Tijerina et al., 2021). Yet, building a large-scale, high-resolution hydrologic model with satisfactory performance remains a challenging task.

The most recent ParFlow CONUS 2.0 (Yang et al., 2023a) surface water-groundwater integrated hydrologic model demonstrates excellent performance in both streamflow and water table depth when compared with substantial observations collected from the USGS and other sources. However, the feasibility of its modeling workflow in other regions of the world has not yet been evaluated. Here, we use the CONUS 2.0 workflow as a starting point to build the modeling platform of continental China (CONCN). China has contrasting climatic conditions, including large arid and semi-arid areas in the northwest with annual potential evapotranspiration up to ~1400 mm (Li et al., 2014) and extremely wet conditions in the southeast with annual precipitation exceeding 2000 mm (Han et al., 2023). The landforms are diverse, encompassing snowpacks, wetlands, deserts, and plains. The dramatic topographic relief is unique, ranging from the world's highest mountain ranges in Tibet to sea level in coastal plains. All these factors make China a favorable testbed for the CONUS 2.0 workflow, yet they also introduce new challenges in modeling. Additionally, US has databases of meteorology, hydrology, topography, soil, and geology, along with relatively mature systems of data management and sharing. In contrast, the existence and accuracy of some necessary data in China remain uncertain. These differences challenge the transferability of the CONUS 2.0 workflow, necessitating modifications during the CONCN modeling process. Hence, building the CONCN model is not only essential for achieving



national-scale consistent management of water resources but also important for identifying the advantages and disadvantages of the workflow. This will help improve the performance of next generation models at larger or global scales.

110 In the following sections, we first introduce the structure and parameters of CONCN 1.0, including the construction of hydrologically consistent topography, hydrostratigraphy, and potential recharge, which are the key components of a ParFlow model. We highlight the challenges in building the CONCN 1.0 model and describe the strategies to overcome these obstacles. We then evaluate the performance of the CONCN model in streamflow and water table depth by both
115 global data products and observations. The comparisons of CONCN model with other model products are not intended to determine which model is better but rather to identify the common problems faced by the modeling community. At the end of the paper, we also discuss the challenges and opportunities in integrated hydrologic modeling for Chinese communities. Note that all performance evaluations in this paper are based on the RSR value which is the ratio of the root
120 mean squared error to the standard deviation of observations. An RSR value of 1.0 suggests good performance while 0.5 suggests excellent performance (O'Neill et al., 2021).

2. Model parameterizations

The CONCN 1.0 model covers the entire continental China (Figure 1a) with a horizontal resolution of 30 arcsec (~1 km at the equator). Vertically, the CONCN model is composed of 10
125 layers with thicknesses of 300, 100, 50, 25, 10, 5, 1, 0.6, 0.3, 0.1 m from bottom to top. This structure results in 4865 and 3927 grid-cells in x and y directions, respectively, and a total of 98.8 million active grid-cells. Although we used the CONUS 2.0 workflow as a starting point for CONCN 1.0, modifications to the workflow were necessary, as mentioned in the introduction. One reason is primarily due to the data availability in China. This does not mean that the relevant data
130 is completely missing, but rather that the data is not readily available for modeling purpose, or that its quality is uncertain. Another reason is due to the scientific progress that has occurred since the development of the CONUS 2.0 model. For example, the total model depth of CONCN 1.0 (492 m) is deeper than that of CONUS 2.0 (392 m). The increased model depth better closes the terrestrial hydrologic cycle, as groundwater contributes to global streamflow to a depth of ~500 m
135 (Ferguson et al., 2023). The details of these modifications are discussed in the following sections.

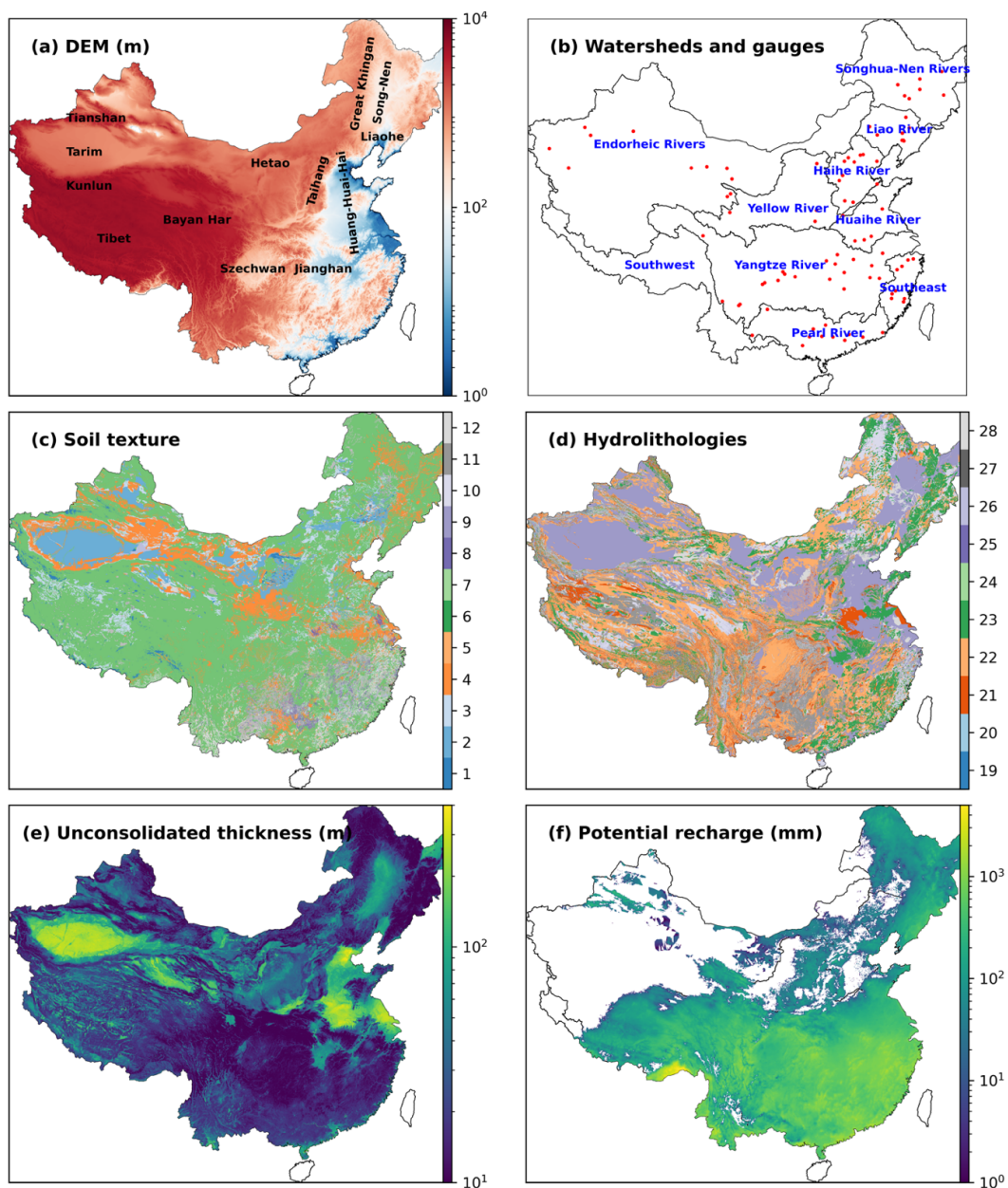


Figure 1. DEM processed by PriorityFlow and labeled with major basins, plains, and mountain ranges (a), major watersheds and streamflow gauges (red points) (b), soil texture of the top soil layer (the first layer from top to bottom) (c), hydrolithologies of the top layer (the fifth layer from top to bottom) (d), unconsolidated thickness (e), and annual potential recharge (f). Indicators of soil texture: 1. Sand, 2. Loamy sand, 3. Sandy loam, 4. Silt loam, 5. Silt, 6. Loam, 7. Sandy clay loam, 8. Silty clay loam, 9. Clay loam, 10. Sandy clay, 11. Silty clay, 12. Clay. Indicators of hydrolithologies: 19. Bedrock 1, 20. Bedrock 2, 21. f.g. sil. sedimentary,

140



145 22. sil. sedimentary, 23. crystalline, 24. f.g. unconsolidated, 25. unconsolidated, 26. c.g. sil
sedimentary, 27. carbonate, 28. c.g. unconsolidated.

2.1. Topographic processing

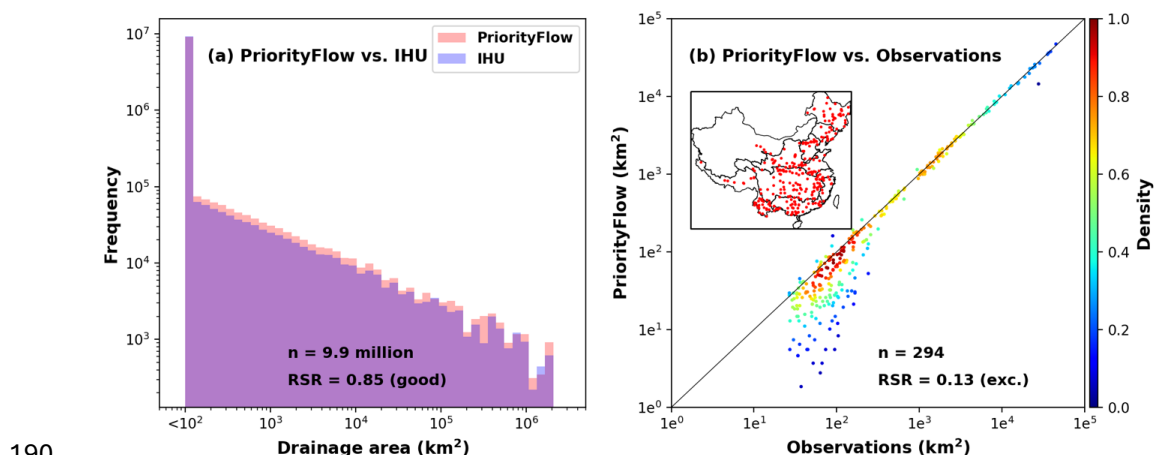
The two most important components of a ParFlow model are the topographic inputs and the hydrostratigraphy, which largely determine the model's performance of streamflow and groundwater, respectively. Since this is a surface water-groundwater integrated hydrologic model, topographic inputs may also influence the potential recharge to groundwater while hydrostratigraphy is crucial for accurate simulations of baseflow. Topographic inputs refer to the slopes in the x and y directions, which are calculated from a digital elevation model (DEM) (Figure 1a). This DEM has been processed to ensure D4 connectivity of the drainage network. D4 connectivity means that streamflow is allowed only in east-west and north-south directions, but not in diagonal directions. The original DEM used in this study is a data product with a resolution of 30 arcsec (Eilander et al., 2021) that was upscaled from the MERIT Hydro DEM with a resolution of 3 arcsec (~90 m at the equator) (Yamazaki et al., 2019), using an Iterative Hydrographic Upscaling approach (hereafter abbreviated as IHU DEM). The DEM was processed using PriorityFlow, which was developed during the CONUS 2.0 modeling (Condon and Maxwell, 2019). Note that the horizontal resolution of the CONCN 1.0 model (i.e., 30 arcsec) is consistent with the resolution of this IHU DEM.

Reference stream networks are preferred as inputs in PriorityFlow to improve drainage performance. The challenge is that we do not have a consistent gridded stream network at the national scale with a resolution close to that of CONCN 1.0, whereas a network with 250 m resolution from the National Water Model (NWM) is available for CONUS 2.0 (Zhang et al., 2021). As a replacement, we generated stream networks from the IHU flow direction of D8 connectivity. Then we checked the generated networks with the vector networks generated from the 3 arcsec MERIT Hydro flow direction (Lin et al., 2019). The initial threshold of drainage area used to generate the input networks from the IHU flow direction was set to 300 km². During processing using PriorityFlow, we refined some networks locally by gradually decreasing the threshold. Such refinements are necessary in areas with flat topography (e.g., the Huang-Huai-Hai plains and coastal plains in Figure 1a), where flow directions are difficult to identify without additional reference networks. Endorheic rivers are common in Northern and Northwest China. Sinks, the end points of these endorheic rivers, are also important to constrain flow directions and thus to



generate accurate stream networks. Manual refinements of stream networks, including the sinks, were iterative processes until the networks generated by PriorityFlow appeared consistent with the vector networks and there were no obvious ponding cells in runoff simulations. A total of 924 sinks were identified in CONCN 1.0, compared to only 131 sinks in CONUS 2.0, which increases the difficulty of the numerical solution, as ParFlow currently does not handle such water bodies.

In addition to the qualitative evaluation described above, we also compared the drainage areas generated by PriorityFlow with that in IHU and 294 observations collected from the literature (Yin et al., 2024). Increasing performance was observed during the iterative processing and the final performances are shown in Figure 2. The PriorityFlow and IHU drainage areas match well, with an RSR value smaller than 1, indicating good performance (Figure 2a). An additional interesting finding is the scaling relationship between drainage areas and frequencies. The comparison with observations shows excellent performance, as the RSR value is smaller than 0.5 (Figure 2b). Deviations from the 1:1 line were observed for drainage areas smaller than 100 km², as we focused more on drainage areas larger than 100 km² during the processing.



190 **Figure 2. Evaluating drainage performance of the topography processed by PriorityFlow using (a) IHU drainage area and (b) observations collected from literature.**

195 2.2. Hydrostratigraphy

The general structure of the hydrostratigraphy is composed of shallow soils and deeper hydroolithologies. The latter includes both unconsolidated and consolidated sediments (Fan et al., 2007; Huscroft et al., 2018). The details of the implementation are as follows: the top 2 m consists



of four soil layers (0.1, 0.4, 0.6 and 1.0 m from top to bottom). The relative percentages of sand,
200 clay, and silt in each layer were derived from a global dataset of soil hydraulic properties (Dai et
al., 2019) with a 30 arcsec resolution. Twelve soil textures (Figure 1c) were then built from these
percentages, based on the soil classification defined by the US Department of Agriculture.
Hydrolithologic categories (Figure 1d) were reclassified from the permeabilities of GLHYMPS
1.0 (Gleeson et al., 2014), which was built by categorizing lithologies in the global lithology map,
205 GLiM. GLiM was compiled by using the geologic map of 1:2.5 million scale in China area released
by the China Geological Survey in 2001 (Hartmann and Moosdorf, 2012). Then *e*-folding,
representing variations in hydraulic conductivity with depth and terrain slope, was applied to each
of the six deep layers (Fan et al., 2007; Tijerina-Kreuzer et al., 2023). Flow barriers (Figure 1e)
were implemented at the interfaces between unconsolidated and consolidated sediments to
210 represent potential confining layers (De graaf et al., 2020; Huscroft et al., 2018). This concept
represents the lumped effects of low-permeability sedimentary materials in the unconsolidated
layer. The dataset we used to represent the interface depths was specifically developed for China
(Yan et al., 2020) and is more accurate than the global version used in CONUS 2.0 (Shangguan et
al., 2017).

215 We adopted this hydrostratigraphy as it is the most convincing scheme from CONUS 2.0,
selected through rigorous hydrologic modeling tests from hundreds of combinations of different
components, such as the distribution of hydrolithologic categories, anisotropy of certain categories,
implementation of confining layers, *e*-folding of hydraulic conductivities, total model depth, and
constant or variable depths of confining layers (i.e., flow barriers) (Swilley et al., 2023; Tijerina-
220 Kreuzer et al., 2023). The hydraulic parameters for each soil texture and hydrolithologic category
(e.g., hydraulic conductivity, porosity, specific yield, and parameters of the van Genuchten model)
were adopted from Schaap and Leij (1998) and Gleeson et al. (2014), with slight calibration in the
CONUS models (Maxwell et al., 2015; Yang et al., 2023a). The parameter configuration assumes
225 that each soil texture or hydrolithologic category has a set of representative, scale-independent
hydraulic parameters.

2.3. Potential recharge

The construction of potential recharge used to drive the model is the most challenging part of
this modeling work. Potential recharge here refers to the multi-year averaged precipitation (P)



minus evapotranspiration (ET), i.e., P-ET. Uncertainties in such hydrometeorological variables are
230 always high. For example, the relative standard deviation (standard deviation relative to the mean)
of the annual mean ET from 12 global products using different approaches reaches 50% (Jiménez
et al., 2011). Given this issue, the P and ET datasets selected for CONUS 2.0 were generated from
a VIC modeling framework (Livneh et al., 2015), which adjusts P for orographic effects and
ensures closure of the land surface water budget. Therefore, uncertainties of all hydrologic
235 variables were constrained within a consistent modeling system. However, datasets of P and ET in
China generated by various approaches have inconsistent uncertainties, and a closed water balance
for all hydrologic components is absent. Uncertainties in P-ET may further accumulate during data
processing (e.g., resampling, interpolations, and transformation) due to differences in the
spatiotemporal resolutions of the P and ET products and the CONCN model. Additionally, record
240 lengths and data quality of some datasets are hard to balance, also challenging the accurate
representation of a long-term average state of the predevelopment condition. We collected four
precipitation products and five ET products generated based on (1) interpolation of measurements
(Han et al., 2023), (2) models including Penman-Monteith equation (Running et al., 2021),
complementary relationship model (Ma et al., 2019), and land surface model (Muñoz-Sabater et
245 al., 2021), and (3) model-data fusion (Huang et al., 2014; Peng, 2020; Niu et al., 2020; Zhang et
al., 2019).

An accurate evaluation of different products was not conducted, as it is beyond the scope of
this study. More importantly, it will take time for the community to gradually improve the quality
of these datasets. We roughly evaluated the products using prior knowledge of some focused areas.
250 For example, we randomly selected several locations and compared the multi-year average levels
of P or ET with the commonly known levels. We used the same approach to evaluate the P-ET
values generated by combining different P and ET datasets. For example, P-ET showed negative
values in some arid and semi-arid regions in northwest China where P-ET should be the dominant
source for known rivers. Although ERA5-Land products also provide P and ET datasets under a
255 consistent modeling framework with high enough resolution (~9 km at the equator), its
precipitation dataset is obviously lower than that constructed using interpolation of substantial
measurements in Han et al. (2023). The best combination of P (Han et al., 2023) and ET (Niu et
al., 2020) in the evaluations was selected to create the average state of potential recharge from
1981 to 2010 (Figure 1f). However, errors induced by uncertainties from P and ET, especially ET,



260 are still evident in some regions, such as the Tarium River Basin, the Heihe River basin, and the
Haihe River Basin (i.e., the North China Plain). The inaccurate estimation of potential recharge
would affect the simulated groundwater and streamflow as discussed in the following sections.

2.4. Manning's coefficients

The Moderate Resolution Imaging Spectroradiometer (MODIS) Land Cover Type (MCD12Q1)
265 version 6.1 data product with a 500 m resolution (Friedl and Sulla-Menashe, 2022) was used to
build the distribution of Manning's coefficients, which are necessary for calculating streamflow,
and will also be required by CLM in the future transient ParFlow-CLM model (Kollet and Maxwell,
2008). The land cover types in this product follow the International Geosphere-Biosphere
Programme (IGBP) classification, which is consistent with the classification required by ParFlow-
270 CLM. In the modeling of CONUS 2.0, a land cover map with a higher resolution of 30 m was
reclassified into the IGBP classification. Some products with resolutions higher than 500 m are
also available in China (Yang and Huang, 2021), but their coarse classification prevented us from
reclassifying the types to subtypes. Stream networks were generated using PriorityFlow with a
threshold drainage area of 50 km², and stream orders were calculated based on the Strahler stream
275 order (Strahler, 1957). Manning's coefficients were set to vary by land cover type and were further
adjusted in stream channels, decreasing in value with increasing stream order.

3. ParFlow modeling platform

ParFlow simulates the movement of 3D variably saturated groundwater and 2D surface water
simultaneously by solving Richards' equation with the shallow water equation as the top boundary
280 (Kollet and Maxwell, 2006). CONCN 1.0 uses a terrain following grid, which significantly reduces
the computational load compared to an orthogonal grid (Maxwell, 2013). The model was
initialized with a uniform water table depth (WTD) of 2 m and was driven by the potential recharge.
All faces of the model, except the top boundary, are no flow boundaries. We ran the model using
the seepage face boundary condition on top of the model until the total storage change was less
285 than 1% of the potential recharge. This is to form the topography-driven patterns of water table.
Afterward, the overland kinematic boundary condition was enabled to generate river systems. The
spinup continued until the total storage change was less than 3% of the potential recharge. River
systems quickly reached a quasi-steady state in groundwater convergence areas, which had already
been identified in the first stage. This two-phase spinup process omitted unnecessary surface water-



290 groundwater interactions during the early stage to improve computational efficiency. Although the dimension of CONCN 1.0 is comparable to CONUS 2.0, CONCN 1.0 required more time for spinup because rivers in arid and semi-arid regions take longer to reach a quasi-steady state, as the water is limitedly recharged by local precipitation but is sourced from the far away upstream.

The Newton-Krylov approach is employed to solve this large nonlinear system, which is
295 discretized on a finite difference grid in an implicit manner. Parallel scalability of the model is ensured by using a multi-grid preconditioner. Thresholds of nonlinear and linear iterations are $1e^{-5}$ and $1e^{-10}$, respectively, to ensure proper convergence. The model was run on the Princeton Della GPU cluster using four 80-GB NVIDIA A100 GPU cards, or on the NCAR Derecho supercomputer using 4096 processor cores across 32 nodes. Each node on Derecho is equipped
300 with 3rd Gen AMD EPYC™ 7763 Milan CPUs.

4. Results and discussion

The simulated streamflow and WTD are shown in Figure 3. Patterns of streamflow (Figure 3a) reveal a contrast between wet and dry regions, generally consistent with the monsoon and non-monsoon regions. Large river systems in the monsoon region are well represented, such as the
305 Yellow River in northern China, the Yangtze River and the Pearl River in southern China, and the Songhua, Nen, and Liao Rivers in northeast China. During the spinup, we observed that the Yellow River is primarily recharged by water sourced from the Bayan Har Mountain ranges and by a small amount of local groundwater. The number of river segments recharged by precipitation increases downstream from the Hetao Plain. River systems in northwest China are also visible, though future
310 work is needed to improve accuracy by reducing uncertainties in potential recharge. The WTD (Figure 3b) presents topography-driven patterns, showing shallow water tables in the Huang-Huai-Hai Plain, the Jiangnan Plain, the Liaohe Basin, and the Songnen Plain. The water table is also shallow inside the Tarim Basin, where the terrain is flat, even though annual precipitation there is less than 50 mm. Deep water tables are distributed along the Tianshan and Kunlun Mountain
315 ranges, the Taihang-Great Khingan Mountain ranges, and the transition area from the Tibet Plateau to the Szechwan Basin.

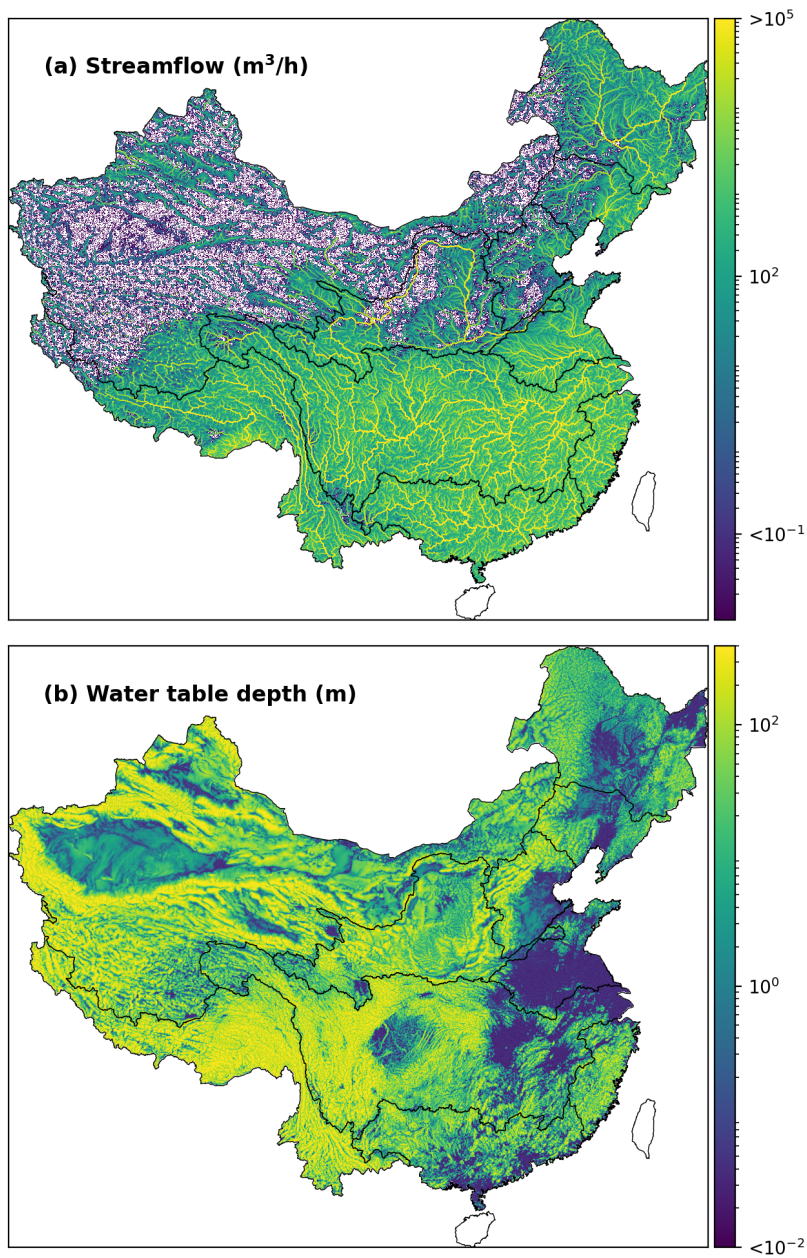


Figure 3. Simulated streamflow and water table depth by CONCN 1.0

The performance of CONCN 1.0 was comprehensively evaluated by both data products and
320 observations. In the evaluation using measured observations, it was difficult to ensure that the
duration of the records was consistent with that of the potential recharge period (1981-2010), as



streamflow or groundwater observations earlier than 2000 are hard to collect. This mismatch between the simulation and observation periods may cause discrepancies between simulated and observed values, due to different drivers resulting from interannual variations of P and ET. This presents a new challenge compared to CONUS 2.0, as publicly available observations in the US date back to around 1900 or even earlier.

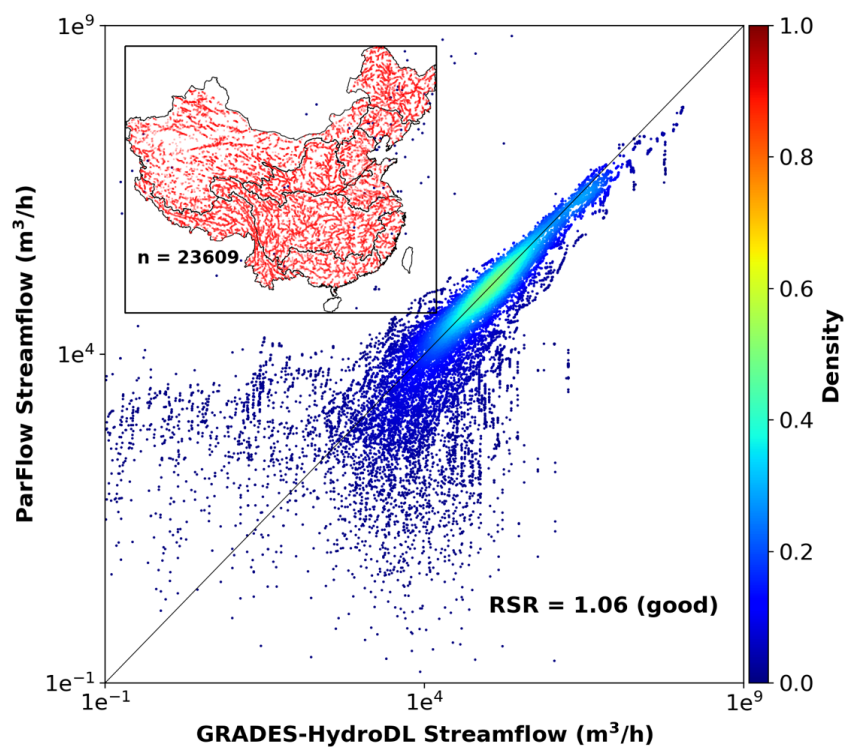
4.1. Evaluation of streamflow

We compared the simulations of CONCN 1.0 with a global streamflow dataset, GRADES-HydroDL (Yang et al., 2023b). The daily streamflow from 1980 to present is estimated for 2.94 million river reaches by applying a Long Short-Term Memory (LSTM) model on a 0.25° grid, developed following Feng et al. (2020), and coupling the LSTM model with a river routing model (RAPID) (David et al., 2011). River reaches with drainage areas larger than 1000 km² were selected, and those with drainage areas larger than 120% or smaller than 80% of the PriorityFlow drainage areas were further filtered out. For each of the selected 23,609 reaches, the streamflow during the potential recharge period (1981 to 2010) was averaged and compared with the simulations of CONCN 1.0. The locations of the selected reaches and a scatterplot of simulations vs. GRADES-HydroDL are shown in Figure 4. Overall, we see a good performance, with an RSR value close to 1. Generally, smaller streamflow values are more scattered in the plot due to the uncertainties associated with smaller drainage areas.

We collected streamflow observations at 95 gauges from the annual River Sediment Bulletin of China, with 88 gauges available for evaluation. Six gauges were removed because we could not find their locations (i.e., latitude and longitude) in the lookup table of national gauges, one of two very close gauges was also removed, and one gauge in Hainan province was excluded as it is outside the modeling domain. The locations of the 88 gauges are shown in Figure 1b, covering most of the modeling domain to ensure an impartial evaluation. However, the number of gauges is obviously limited, and augmenting the database for this modeling platform will take time. The observations include monthly records spanning from 2002 to 2021. Although most gauges do not have a complete 20-year record, each gauge has at least a two-year record. Scatterplots of simulations vs. observations are shown in Figure 5. Most basins show good to excellent performance, with RSR values close to 1.0 or 0.5. Simulated streamflow of the Endorheic, Haihe and part of the Liao Rivers is much lower than observed. This is likely due to uncertainties in

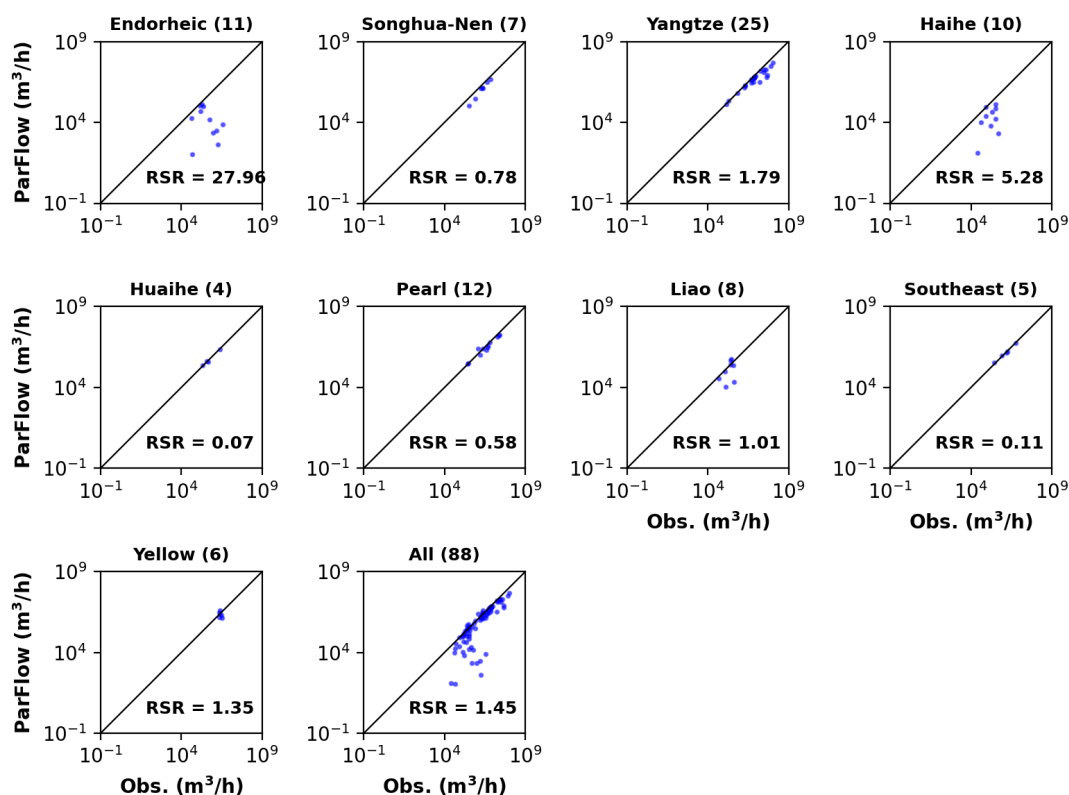


potential recharge, as discussed in section 2.3, and the fact that simulations at these gauges are mainly baseflow sourced from groundwater. Slight deviations are also seen along the mainstream of the Yangtze and Yellow Rivers, likely caused by hydraulic engineering, such as dam operations.



355

Figure 4. Scatterplot of simulated streamflow vs. GRADES-HydroDL. Locations of the selected reaches for comparison are shown in the upper left corner.



360

Figure 5. Scatterplots of simulated vs. observed streamflow

4.2. Evaluation of water table depth

Steady-state WTDs generated by two global groundwater models were collected (Figures 6a-
365 b). Both global models have a horizontal resolution of 30 arcsec, but their formulations and vertical
structures differ significantly from CONCN 1.0. The first model is a horizontal, two-dimensional
groundwater model based on water balance and Darcy's law, developed by Fan et al. (2013). This
model was driven by soil drainage from global land models at the water table. The second model,
GLOBGM v1.0, refined the 5 arcmin PCR-GLOBWB-MODFLOW (De Graaf et al., 2015; De
370 Graaf et al., 2017), which is a two-layer, three-dimensional groundwater model driven by the
output from PCR-GLOBWB (Verkaik et al., 2024).

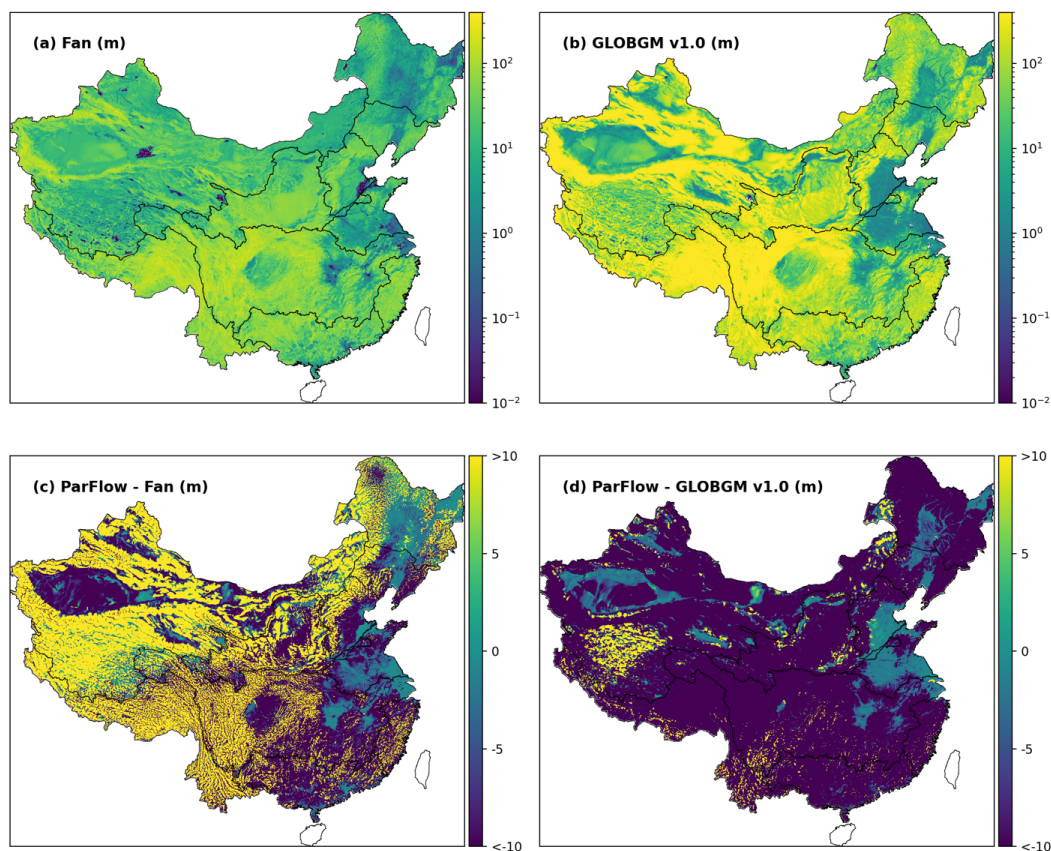


Figure 6. Water table depths from two global models in China area (a-b) and the differences between CONCN 1.0 and these two models (c-d).

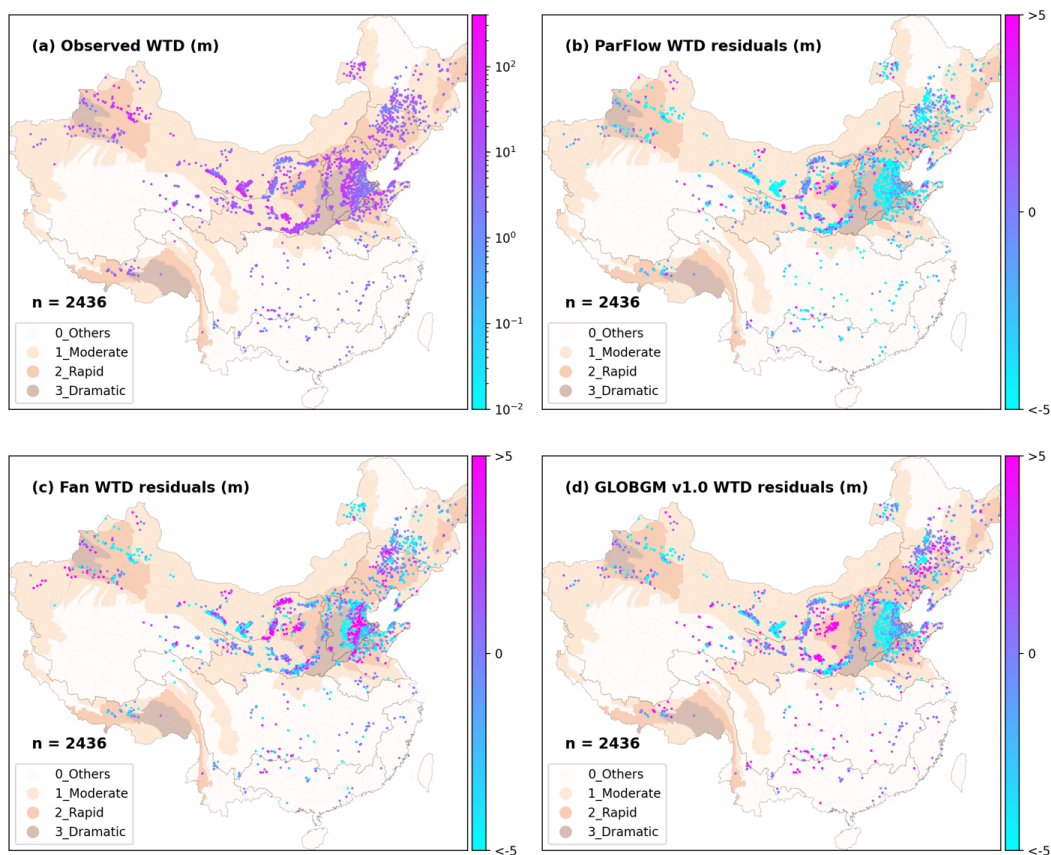
375

We collected monthly observations of hydraulic head in 8563 wells in 2018. After removing wells located outside the model domain, in confined aquifers, and on ParFlow channels, 2436 wells remained for evaluation (Figure 7a). The annual means of WTD were calculated based on well elevations measured at the land surface. These wells are part of the national groundwater monitoring network maintained by the Ministry of Land and Resources. We collected the data by digitizing the China Geological Environmental Monitoring Groundwater Level Yearbook of 2018 and then double-checked the data to avoid errors. The yearbook, which started from 2005, has currently been updated to 2021. We fully understand that one-year monthly observations cannot represent the long-term average state of the water table. An ongoing effort is being made to digitize

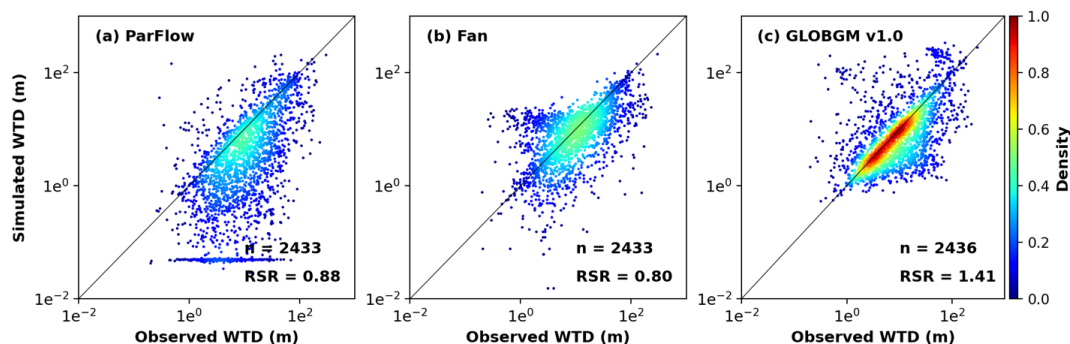
380



385 all the data in the yearbook and apply QA/QC (quality assurance and quality control) on the
digitized data, although it will take a few years to complete.



390 **Figure 7. Well locations (a) and residuals of water table depth for each model (b-d). The background shows the average decrease of groundwater storage from 2003 to 2020 based on GRACE data (Zhao et al., 2023). The decrease is classified into three levels: moderate, rapid, and dramatic.**



395 **Figure 8. Scatterplots of simulations vs. observations of water table depth.**

We then compared WTDs simulated by three models with observations (Figure 8). RSR values show generally good performances of all three models and indicate that the performance of CONCEN 1.0 is intermediate between the two global models (0.88, compared to 0.80 and 1.41).
400 However, we observe a shift toward shallower water tables simulated by CONCEN 1.0. The residuals of WTD for each model are shown in Figures 7b-d. Each subplot also shows the decrease of groundwater storage based on GRACE data (Zhao et al., 2023), which is classified into three levels: moderate, rapid, and dramatic. A decrease of groundwater storage is mainly observed in Northern China, such as the Song-Liao Plains, the North China Plain, the Hetao Plain, and the northern edge of Tarim Basin. Agriculture is well-developed in these areas, with intensive groundwater pumping for irrigation. While the model simulations represent natural conditions without groundwater pumping, simulated water tables are expected to be shallower than observed, resulting in negative WTD residuals. However, the residuals from Fan's model show substantial positive residuals in these areas (Figure 7c). Similarly, positive residuals of GLOBGM v1.0 are found in Tibet and the Song-Liao Plains, where the decrease of groundwater storage is significant.
405 It is important to note that both Fan's model and GLOBGM v1.0 are calibrated models while the ParFlow CONCEN 1.0 model is not. Therefore, further calibrations of global models are necessary to better represent the natural conditions of WTD in space. All three models show deep simulated water tables just below the Szechwan Basin, at the boundaries of the Yangtze River and Pearl River Basins. This may suggest a higher recharge in 2018 compared to the historic period (1981-2010),
415 which was used to drive the models.



In wet southern China, CONCN 1.0 and Fan's model show similar shallow water tables, while GLOBGW v1.0 shows relatively deeper ones (Figures 7b-d). These differences may originate from the different model formulations. ParFlow integrates overland flow and groundwater movement by solving Richards' and shallow water equations simultaneously via shared nodes in the top layer. As a result, WTDs in many wells close to rivers are likely underestimated due to the widened rivers in the model, which has a 1 km resolution. WTDs in some wells located tens or hundreds of meters from rivers cannot even be captured, as the grid-cell is already fully saturated. However, monitoring wells are commonly distributed close to rivers, which explains the shallow simulations by CONCN 1.0 in southern China (Figure 7b). Fan's model removed groundwater that converged in river channels, so water tables in southern China are slightly deeper than that in CONCN 1.0 but not much (Figure 7c). GLOBGW v1.0 includes river-groundwater interactions by the difference between the groundwater head and river level, but rivers and the top subsurface layer are loosely coupled, without shared pressure heads. In other words, groundwater may discharge to rivers when its level is lower than the land surface. Additionally, WTDs, even in grid-cells with rivers, can be calibrated, which is not possible in ParFlow due to its integrated formulation. To avoid bias in evaluation caused by well locations, we plotted the differences of WTDs between CONCN 1.0 and two global models in Figures 6c-d. We find that Fan's model generally shows shallower WTDs while GLOBGW v1.0 shows deeper WTDs, even in southern China, expanding the evaluations based on observations only. The significant differences of WTDs across three models also imply high uncertainties in WTDs simulated by current large-scale groundwater models which cannot be fully captured by limited observations. Further efforts on parameterizations and formulations of the models are needed from this modeling community.

4.3. Challenges and opportunities going forward

We hope that our work can catalyze conversation and collaboration between various communities involved in hydrologic modeling, geologic surveys, model development, data products, and data monitoring/sharing. Clearly, all efforts are aimed at improving the efficiencies and capabilities of large-scale hydrologic modeling to address different ecohydrologic issues and accelerate the scientific discoveries across multiple disciplines. We have summarized the challenges, but also the opportunities, below-these require the attention and collaborative efforts of the hydrology community and many others.



- 450 (1) Human activities relevant to water resources are intensive in China, such as the groundwater depletion due to the long-term groundwater pumping in Huang-Huai-Hai plains, the South-North water transfer projects, the operations of the Three Gorges Dam, and the revegetation in the Loess Plateau. Flash extremes are also becoming more frequent, such as the Yangtze drought in August 2022 and the storms in Zhengzhou in July 2022 and Beijing in July 2023. All of these factors make China one of the most significant ecohydrologic hotspots in the world. Integrated hydrologic modeling systems are essential to address these issues. Though local and regional models have been developed in recent
- 455 years, modeling platforms with high resolutions at larger or national scales are still absent, hindering the efficient water resources management and timely decision-making across multiple scales.
- 460 (2) Hydrologic processes, especially groundwater at hillslope or catchment scales, play important roles in terrestrial water and energy cycles, yet they have often been simplified and are not well represented in Earth system models. Many studies conducted in China on critical questions have focused on limited components of the hydrologic cycle. Therefore, it is urgent to build large-scale hydrologic models and couple them with regional weather or climatic models to better understand the terrestrial hydrologic cycle in China. More importantly, the modeling should go beyond water balance to include flow paths or water
- 465 quality to gain a deeper understanding of the food-energy-water nexus and to conduct risk assessments in the changing world.
- 470 (3) Large-scale hydrologic modeling relies on massive amounts of data for different input variables. Discrete observations are not user-friendly for direct use by modelers. Data products help fill spatial and temporal gaps and are essential for modeling. Many of the products we have used only emerged in recent years, making it impossible to conduct large-scale hydrologic modeling efficiently in China and many other places in the world in earlier years. The rapid development of global data products suggests that now it is the right time to build large-scale, consistent hydrologic modeling platforms. However, high quality data products within a consistent framework are still lacking and inter-evaluations between
- 475 different products might be a way to constrain uncertainties from various sources (see section 2.3).



(4) We also need to leverage the advantages of local documents in China. The hydrogeologies of GLHYMPS 1.0 were built on the global lithology map GLiM, which, in turn, used the geological map with a scale of 1:2.5 million published by China Geological Survey in 2001. Currently, national geological maps with a scale of 1:500,000 are available, while some local maps have the scale to 1:50,000. We need to fully consider such materials to improve the permeability/hydrogeology products in China in terms of both horizontal resolution and available depth. This is critical for building a more reliable hydrostratigraphy, which could substantially improve the model's performance. Beyond permeability, any regions with other more detailed local measurements should also be utilized to evaluate and improve current modeling formulations.

(5) Large-scale hydrologic models built using different formulations are encouraged. Model comparisons are necessary to identify the strengths and weaknesses of different modeling systems on focused issues. Such community activities are also helpful in reaching agreements on critical questions, such as conceptual models or model parameterizations, calibrations, evaluations, and the opportunities to incorporate new techniques and concepts. All of these factors are important for improving the performance of next generation models in China and can provide useful references and inspiration for modeling efforts in other places in the world.

5. Conclusions

In this study, we built the first surface water-groundwater integrated hydrologic modeling platform of the entire continental China with a high resolution using ParFlow. This CONCN 1.0 model was rigorously evaluated by both data products and observations, based on RSR values. Comparisons with observations show good to excellent performance in streamflow and water table depth. Comparisons with global data products show comparable performance of streamflow to the global model and an intermediate performance of water table depth among global models. These results also demonstrate the transferability of the modeling workflow using ParFlow. However, we also recognize the deficiency of this modeling platform. Data quality and/or availability (e.g., for direct use or quick access) presents a significant challenge during modeling. The vast arid and semi-arid regions of China further increase uncertainties in input data, such as potential recharge. As a result, lower simulated streamflow is observed in northwest China and in the Haihe and Liao



River Basins. Significant uncertainties in simulated water table depth are identified in current large-scale groundwater models, which might be attributed to the different parameterizations and formulations of the models, necessitating continuous efforts from the community. We also discussed opportunities in hydrologic modeling in China based on the country's current ecohydrologic situation and the challenges encountered in modeling, which may also inspire similar modeling efforts in other places with conditions similar to those of China.

Data and code availability

Datasets we used are all from public sources and have cited in the main text. The ParFlow Version 3.12-3.13 we used can be found here: <https://doi.org/10.5281/zenodo.4816884>

Author contributions

Conceptualization: CY and RM. Methodology: CY, LC, and RM. Investigation: CY, ZJ, WX, and RM. Resources: ZW, XZ, YZ, YD, and RM. Writing – original draft: CY. Writing – review and editing: CY, JM, and RM.

Competing interests

The contact author has declared that none of the authors has any competing interests.

Acknowledgements

We are pleased to acknowledge that the work reported on in this paper was substantially performed using the Princeton Research Computing resources at Princeton University which is consortium of groups led by the Princeton Institute for Computational Science and Engineering (PICSciE) and Office of Information Technology's Research Computing. We would like to acknowledge high-performance computing support from Cheyenne (doi:10.5065/D6RX99HX) provided by NCAR's Computational and Information Systems Laboratory, sponsored by the National Science Foundation.

References

Belleflamme, A., Goergen, K., Wagner, N., Kollet, S., Bathiany, S., El Zohbi, J., Rechid, D., Vanderborght, J., and Vereecken, H.: Hydrological forecasting at impact scale: the integrated ParFlow hydrological model at 0.6 km for climate resilient water resource management over Germany, *Frontiers in Water*, 5, 10.3389/frwa.2023.1183642, 2023.
Bianchi, M., Scheidegger, J., Hughes, A., Jackson, C., Lee, J., Lewis, M., Mansour, M., Newell, A., O'Dochartaigh, B., Patton, A., and Dadson, S.: Simulation of national-scale



- groundwater dynamics in geologically complex aquifer systems: an example from Great
Britain, *Hydrological Sciences Journal*, 69, 572-591, 10.1080/02626667.2024.2320847,
540 2024.
- Cao, G. L., Zheng, C. M., Scanlon, B. R., Liu, J., and Li, W. P.: Use of flow modeling to assess
sustainability of groundwater resources in the North China Plain, *Water Resour Res*, 49,
159-175, 10.1029/2012wr011899, 2013.
- Chen, J., Sudicky, E. A., Davison, J. H., Frey, S. K., Park, Y. J., Hwang, H. T., Erler, A. R., Berg,
545 S. J., Callaghan, M. V., Miller, K., Ross, M., and Peltier, W. R.: Towards a climate-driven
simulation of coupled surface-subsurface hydrology at the continental scale: a Canadian
example, *Canadian Water Resources Journal / Revue canadienne des ressources
hydriques*, 45, 11-27, 10.1080/07011784.2019.1671235, 2020.
- Collins, G. and Reddy, G.: China's Growing Water Crisis, *Foreign Affairs*, 2022.
- 550 Condon, L. E. and Maxwell, R. M.: Modified priority flood and global slope enforcement
algorithm for topographic processing in physically based hydrologic modeling applications,
Comput Geosci-Uk, 126, 73-83, 10.1016/j.cageo.2019.01.020, 2019.
- Condon, L. E., Kollet, S., Bierkens, M. F. P., Fogg, G. E., Maxwell, R. M., Hill, M. C., Fransen,
H.-J. H., Verhoef, A., Van Loon, A. F., Sulis, M., and Abesser, C.: Global Groundwater
555 Modeling and Monitoring: Opportunities and Challenges, *Water Resour Res*, 57,
e2020WR029500, <https://doi.org/10.1029/2020WR029500>, 2021.
- Cosgrove, B., Gochis, D., Flowers, T., Dugger, A., Ogden, F., Graziano, T., Clark, E., Cabell,
R., Casiday, N., Cui, Z., Eicher, K., Fall, G., Feng, X., Fitzgerald, K., Frazier, N., George, C.,
Gibbs, R., Hernandez, L., Johnson, D., Jones, R., Karsten, L., Kefelegn, H., Kitzmiller, D.,
560 Lee, H., Liu, Y., Mashriqui, H., Mattern, D., McCluskey, A., McCreight, J. L., McDaniel, R.,
Midekisa, A., Newman, A., Pan, L., Pham, C., RafieeiNasab, A., Rasmussen, R., Read, L.,
Rezaeianzadeh, M., Salas, F., Sang, D., Sampson, K., Schneider, T., Shi, Q., Sood, G., Wood,
A., Wu, W., Yates, D., Yu, W., and Zhang, Y.: NOAA's National Water Model: Advancing
operational hydrology through continental-scale modeling, *JAWRA Journal of the American
565 Water Resources Association*, 60, 247-272, <https://doi.org/10.1111/1752-1688.13184>,
2024.
- Dai, Y., Xin, Q., Wei, N., Zhang, Y., Shangguan, W., Yuan, H., Zhang, S., Liu, S., and Lu, X.: A
Global High-Resolution Data Set of Soil Hydraulic and Thermal Properties for Land Surface
Modeling, *J Adv Model Earth Sy*, 11, 2996-3023, <https://doi.org/10.1029/2019MS001784>,
570 2019.
- David, C. H., Maidment, D. R., Niu, G.-Y., Yang, Z.-L., Habets, F., and Eijkhout, V.: River
Network Routing on the NHDPlus Dataset, *J Hydrometeorol*, 12, 913-934,
<https://doi.org/10.1175/2011JHM1345.1>, 2011.
- de Graaf, I., Condon, L., and Maxwell, R.: Hyper-Resolution Continental-Scale 3-D Aquifer
575 Parameterization for Groundwater Modeling, *Water Resour Res*, 56, e2019WR026004,
<https://doi.org/10.1029/2019WR026004>, 2020.
- de Graaf, I. E. M., Sutanudjaja, E. H., van Beek, L. P. H., and Bierkens, M. F. P.: A high-
resolution global-scale groundwater model, *Hydrol Earth Syst Sc*, 19, 823-837,
10.5194/hess-19-823-2015, 2015.
- 580 de Graaf, I. E. M., van Beek, R. L. P. H., Gleeson, T., Moosdorf, N., Schmitz, O., Sutanudjaja,
E. H., and Bierkens, M. F. P.: A global-scale two-layer transient groundwater model:



- Development and application to groundwater depletion, *Adv Water Resour*, 102, 53-67, <https://doi.org/10.1016/j.advwatres.2017.01.011>, 2017.
- 585 Delsman, J. R., Mulder, T., Romero Verastegui, B., Bootsma, H., Zitman, P., Huizer, S., and Oude Essink, G. H. P.: Reproducible construction of a high-resolution national variable-density groundwater salinity model for the Netherlands, *Environ Modell Softw*, 164, 105683, <https://doi.org/10.1016/j.envsoft.2023.105683>, 2023.
- 590 Eilander, D., van Verseveld, W., Yamazaki, D., Weerts, A., Winsemius, H. C., and Ward, P. J.: A hydrography upscaling method for scale-invariant parametrization of distributed hydrological models, *Hydrol. Earth Syst. Sci.*, 25, 5287-5313, 10.5194/hess-25-5287-2021, 2021.
- Fan, Y., Li, H., and Miguez-Macho, G.: Global Patterns of Groundwater Table Depth, *Science*, 339, 940-943, 10.1126/science.1229881, 2013.
- 595 Fan, Y., Miguez-Macho, G., Weaver, C. P., Walko, R., and Robock, A.: Incorporating water table dynamics in climate modeling: 1. Water table observations and equilibrium water table simulations, *Journal of Geophysical Research: Atmospheres*, 112, <https://doi.org/10.1029/2006JD008111>, 2007.
- Feng, D., Fang, K., and Shen, C.: Enhancing Streamflow Forecast and Extracting Insights Using Long-Short Term Memory Networks With Data Integration at Continental Scales, *Water Resour Res*, 56, e2019WR026793, <https://doi.org/10.1029/2019WR026793>, 2020.
- 600 Ferguson, G., McIntosh, J. C., Jasechko, S., Kim, J.-H., Famiglietti, J. S., and McDonnell, J. J.: Groundwater deeper than 500 m contributes less than 0.1% of global river discharge, *Commun Earth Environ*, 4, 48, 10.1038/s43247-023-00697-6, 2023.
- Friedl, M. and Sulla-Menashe, D.: MODIS/Terra+Aqua Land Cover Type Yearly L3 Global 500m SIN Grid V061, NASA EOSDIS Land Processes Distributed Active Archive Center [dataset], <https://doi.org/10.5067/MODIS/MCD12Q1.061>, 2022.
- 605 Gleeson, T., Moosdorf, N., Hartmann, J., and van Beek, L. P. H.: A glimpse beneath earth's surface: GLobal HYdrogeology MaPS (GLHYMPS) of permeability and porosity, *Geophys Res Lett*, 41, 3891-3898, 10.1002/2014gl059856, 2014.
- 610 Gleeson, T., Wagener, T., Döll, P., Zipper, S. C., West, C., Wada, Y., Taylor, R., Scanlon, B., Rosolem, R., Rahman, S., Oshinlaja, N., Maxwell, R., Lo, M. H., Kim, H., Hill, M., Hartmann, A., Fogg, G., Famiglietti, J. S., Ducharne, A., de Graaf, I., Cuthbert, M., Condon, L., Bresciani, E., and Bierkens, M. F. P.: GMD perspective: The quest to improve the evaluation of groundwater representation in continental- to global-scale models, *Geosci. Model Dev.*, 14, 7545-7571, 10.5194/gmd-14-7545-2021, 2021.
- 615 Han, J., Miao, C., Gou, J., Zheng, H., Zhang, Q., and Guo, X.: A new daily gridded precipitation dataset for the Chinese mainland based on gauge observations, *Earth Syst. Sci. Data*, 15, 3147-3161, 10.5194/essd-15-3147-2023, 2023.
- 620 Hartmann, J. and Moosdorf, N.: The new global lithological map database GLiM: A representation of rock properties at the Earth surface, *Geochemistry, Geophysics, Geosystems*, 13, <https://doi.org/10.1029/2012GC004370>, 2012.
- Hellwig, J., de Graaf, I. E. M., Weiler, M., and Stahl, K.: Large-Scale Assessment of Delayed Groundwater Responses to Drought, *Water Resour Res*, 56, e2019WR025441, <https://doi.org/10.1029/2019WR025441>, 2020.



- 625 Henriksen, H. J., Troldborg, L., Nyegaard, P., Sonnenborg, T. O., Refsgaard, J. C., and Madsen, B.: Methodology for construction, calibration and validation of a national hydrological model for Denmark, *J Hydrol*, 280, 52-71, [https://doi.org/10.1016/S0022-1694\(03\)00186-0](https://doi.org/10.1016/S0022-1694(03)00186-0), 2003.
- Hoch, J. M., Sutanudjaja, E. H., Wanders, N., van Beek, R. L. P. H., and Bierkens, M. F. P.: Hyper-resolution PCR-GLOBWB: opportunities and challenges from refining model spatial resolution to 1 km over the European continent, *Hydrol. Earth Syst. Sci.*, 27, 1383-1401, 10.5194/hess-27-1383-2023, 2023.
- 630 Hu, L., Xu, Z., and Huang, W.: Development of a river-groundwater interaction model and its application to a catchment in Northwestern China, *J Hydrol*, 543, 483-500, <https://doi.org/10.1016/j.jhydrol.2016.10.028>, 2016.
- 635 Huang, C., Zheng, X., Tait, A., Dai, Y., Yang, C., Chen, Z., Li, T., and Wang, Z.: On using smoothing spline and residual correction to fuse rain gauge observations and remote sensing data, *J Hydrol*, 508, 410-417, <https://doi.org/10.1016/j.jhydrol.2013.11.022>, 2014.
- 640 Huscroft, J., Gleeson, T., Hartmann, J., and Börker, J.: Compiling and Mapping Global Permeability of the Unconsolidated and Consolidated Earth: GLObal HYdrogeology MaPS 2.0 (GLHYMPS 2.0), *Geophys Res Lett*, 45, 1897-1904, <https://doi.org/10.1002/2017GL075860>, 2018.
- Jiang, X., Ma, R., Ma, T., and Sun, Z.: Modeling the effects of water diversion projects on surface water and groundwater interactions in the central Yangtze River basin, *Sci Total Environ*, 830, 154606, <https://doi.org/10.1016/j.scitotenv.2022.154606>, 2022.
- 645 Jiang, Y.: China's water scarcity, *Journal of Environmental Management*, 90, 3185-3196, <https://doi.org/10.1016/j.jenvman.2009.04.016>, 2009.
- Jiménez, C., Prigent, C., Mueller, B., Seneviratne, S. I., McCabe, M. F., Wood, E. F., Rossow, W. B., Balsamo, G., Betts, A. K., Dirmeyer, P. A., Fisher, J. B., Jung, M., Kanamitsu, M., Reichle, R. H., Reichstein, M., Rodell, M., Sheffield, J., Tu, K., and Wang, K.: Global intercomparison of 12 land surface heat flux estimates, *Journal of Geophysical Research: Atmospheres*, 116, <https://doi.org/10.1029/2010JD014545>, 2011.
- 650 Kollet, S. J. and Maxwell, R. M.: Integrated surface-groundwater flow modeling: A free-surface overland flow boundary condition in a parallel groundwater flow model, *Adv Water Resour*, 29, 945-958, 2006.
- 655 Kollet, S. J. and Maxwell, R. M.: Capturing the influence of groundwater dynamics on land surface processes using an integrated, distributed watershed model, *Water Resour Res*, 44, Artn W0240210.1029/2007wr006004, 2008.
- Lancia, M., Yao, Y., Andrews, C. B., Wang, X., Kuang, X., Ni, J., Gorelick, S. M., Scanlon, B. R., Wang, Y., and Zheng, C.: The China groundwater crisis: A mechanistic analysis with implications for global sustainability, *Sustainable Horizons*, 4, 100042, <https://doi.org/10.1016/j.horiz.2022.100042>, 2022.
- 660 Li, Z., Chen, Y., Yang, J., and Wang, Y.: Potential evapotranspiration and its attribution over the past 50 years in the arid region of Northwest China, *Hydrol Process*, 28, 1025-1031, <https://doi.org/10.1002/hyp.9643>, 2014.
- 665 Lin, P., Pan, M., Beck, H. E., Yang, Y., Yamazaki, D., Frasson, R., David, C. H., Durand, M., Pavelsky, T. M., Allen, G. H., Gleason, C. J., and Wood, E. F.: Global Reconstruction of



- Naturalized River Flows at 2.94 Million Reaches, *Water Resour Res*, 55, 6499-6516, 10.1029/2019wr025287, 2019.
- 670 Livneh, B., Bohn, T. J., Pierce, D. W., Munoz-Arriola, F., Nijssen, B., Vose, R., Cayan, D. R., and Brekke, L.: A spatially comprehensive, hydrometeorological data set for Mexico, the U.S., and Southern Canada 1950–2013, *Sci Data*, 2, 150042, 10.1038/sdata.2015.42, 2015.
- Ma, N., Szilagyi, J., Zhang, Y., and Liu, W.: Complementary-Relationship-Based Modeling of Terrestrial Evapotranspiration Across China During 1982–2012: Validations and
- 675 Spatiotemporal Analyses, *Journal of Geophysical Research: Atmospheres*, 124, 4326-4351, <https://doi.org/10.1029/2018JD029850>, 2019.
- Maxwell, R. M.: A terrain-following grid transform and preconditioner for parallel, large-scale, integrated hydrologic modeling, *Adv Water Resour*, 53, 109-117, <https://doi.org/10.1016/j.advwatres.2012.10.001>, 2013.
- 680 Maxwell, R. M., Condon, L. E., and Kollet, S. J.: A high-resolution simulation of groundwater and surface water over most of the continental US with the integrated hydrologic model ParFlow v3, *Geosci Model Dev*, 8, 923-937, 10.5194/gmd-8-923-2015, 2015.
- Miao, C., Gou, J., Fu, B., Tang, Q., Duan, Q., Chen, Z., Lei, H., Chen, J., Guo, J., Borthwick, A. G. L., Ding, W., Duan, X., Li, Y., Kong, D., Guo, X., and Wu, J.: High-quality reconstruction of
- 685 China's natural streamflow, *Science Bulletin*, 67, 547-556, <https://doi.org/10.1016/j.scib.2021.09.022>, 2022.
- Muñoz-Sabater, J., Dutra, E., Agustí-Panareda, A., Albergel, C., Arduini, G., Balsamo, G., Boussetta, S., Choulga, M., Harrigan, S., Hersbach, H., Martens, B., Miralles, D. G., Piles, M., Rodríguez-Fernández, N. J., Zsoter, E., Buontempo, C., and Thépaut, J. N.: ERA5-Land: a
- 690 state-of-the-art global reanalysis dataset for land applications, *Earth Syst. Sci. Data*, 13, 4349-4383, 10.5194/essd-13-4349-2021, 2021.
- Niu, Z., He, H., Zhu, G., Ren, X., Zhang, L., and Zhang, K.: A spatial-temporal continuous dataset of the transpiration to evapotranspiration ratio in China from 1981–2015, *Sci Data*, 7, 369, 10.1038/s41597-020-00693-x, 2020.
- 695 O'Neill, M. M. F., Tijerina, D. T., Condon, L. E., and Maxwell, R. M.: Assessment of the ParFlow-CLM CONUS 1.0 integrated hydrologic model: evaluation of hyper-resolution water balance components across the contiguous United States, *Geosci. Model Dev.*, 14, 7223-7254, 10.5194/gmd-14-7223-2021, 2021.
- Peng, S.: 1-km monthly precipitation dataset for China (1901-2022), National Tibetan
- 700 Plateau Data Center [dataset], 10.5281/zenodo.3185722, 2020.
- Pietz, D. A.: China's Water Challenges: National and Global Implications, *Education About ASIA*, 22, 8-14, 2017.
- Regan, R. S., Juracek, K. E., Hay, L. E., Markstrom, S. L., Viger, R. J., Driscoll, J. M., LaFontaine, J. H., and Norton, P. A.: The U. S. Geological Survey National Hydrologic Model
- 705 infrastructure: Rationale, description, and application of a watershed-scale model for the conterminous United States, *Environ Modell Softw*, 111, 192-203, <https://doi.org/10.1016/j.envsoft.2018.09.023>, 2019.
- Reinecke, R., Foglia, L., Mehl, S., Trautmann, T., Cáceres, D., and Döll, P.: Challenges in developing a global gradient-based groundwater model (G3M v1.0) for the integration into a
- 710 global hydrological model, *Geosci. Model Dev.*, 12, 2401-2418, 10.5194/gmd-12-2401-2019, 2019.



- Reinecke, R., Wachholz, A., Mehl, S., Foglia, L., Niemann, C., and Döll, P.: Importance of Spatial Resolution in Global Groundwater Modeling, *Groundwater*, 58, 363-376, <https://doi.org/10.1111/gwat.12996>, 2020.
- 715 Running, S., Mu, Q., Zhao, M., and Moreno, A.: MODIS/Terra Net Evapotranspiration Gap-Filled Yearly L4 Global 500m SIN Grid V061, NASA EOSDIS Land Processes Distributed Active Archive Center [dataset], <https://doi.org/10.5067/MODIS/MOD16A3GF.061>, 2021.
- Schaap, M. G. and Leij, F. J.: Database-related accuracy and uncertainty of pedotransfer functions, *Soil science*, v. 163, pp. 765-779-1998 v.1163 no.1910, 10.1097/00010694-199810000-00001, 1998.
- 720 Schmied, H., Cáceres, D., Eisner, S., Flörke, M., Herbert, C., Niemann, C., Peiris, T. A., Popat, E., Portmann, F. T., Reinecke, R., Schumacher, M., Shadkam, S., Telteu, C. E., Trautmann, T., and Döll, P.: The global water resources and use model WaterGAP v2.2d: model description and evaluation, *Geosci. Model Dev.*, 14, 1037-1079, 10.5194/gmd-14-1037-2021, 2021.
- 725 Shangguan, W., Hengl, T., de Jesus, J. M., Yuan, H., and Dai, Y. J.: Mapping the global depth to bedrock for land surface modeling, *J Adv Model Earth Sy*, 9, 65-88, 2017.
- Strahler, A. N.: Quantitative analysis of watershed geomorphology, *Eos, Transactions American Geophysical Union*, 38, 913-920, <https://doi.org/10.1029/TR038i006p00913>, 1957.
- 730 Sutanudjaja, E. H., van Beek, R., Wanders, N., Wada, Y., Bosmans, J. H. C., Drost, N., van der Ent, R. J., de Graaf, I. E. M., Hoch, J. M., de Jong, K., Karssenberg, D., López López, P., Peßenteiner, S., Schmitz, O., Straatsma, M. W., Vannamettee, E., Wisser, D., and Bierkens, M. F. P.: PCR-GLOBWB 2: a 5 arcmin global hydrological and water resources model, *Geosci. Model Dev.*, 11, 2429-2453, 10.5194/gmd-11-2429-2018, 2018.
- 735 Swilley, J. S., Tijerina-Kreuzer, D., Tran, H. V., Zhang, J., Yang, C., Condon, L. E., and Maxwell, R. M.: Continental Scale Hydrostratigraphy: Comparing Geologically Informed Data Products to Analytical Solutions, *Groundwater*, n/a, <https://doi.org/10.1111/gwat.13354>, 2023.
- 740 Tian, Y., Zheng, Y., Zheng, C., Xiao, H., Fan, W., Zou, S., Wu, B., Yao, Y., Zhang, A., and Liu, J.: Exploring scale-dependent ecohydrological responses in a large endorheic river basin through integrated surface water-groundwater modeling, *Water Resour Res*, 51, 4065-4085, <https://doi.org/10.1002/2015WR016881>, 2015.
- 745 Tijerina, D., Condon, L., FitzGerald, K., Dugger, A., O'Neill, M. M., Sampson, K., Gochis, D., and Maxwell, R.: Continental Hydrologic Intercomparison Project, Phase 1: A Large-Scale Hydrologic Model Comparison Over the Continental United States, *Water Resour Res*, 57, e2020WR028931, <https://doi.org/10.1029/2020WR028931>, 2021.
- Tijerina-Kreuzer, D., Swilley, J. S., Tran, H. V., Zhang, J., West, B., Yang, C., Condon, L. E., and Maxwell, R. M.: Continental scale hydrostratigraphy: basin-scale testing of alternative data-driven approaches, *Groundwater*, n/a, <https://doi.org/10.1111/gwat.13357>, 2023.
- 750 Vergnes, J.-P., Caballero, Y., and Lanini, S.: Assessing climate change impact on French groundwater resources using a spatially distributed hydrogeological model, *Hydrological Sciences Journal*, 68, 209-227, 10.1080/02626667.2022.2150553, 2023.
- 755 Verkaik, J., Sutanudjaja, E. H., Oude Essink, G. H. P., Lin, H. X., and Bierkens, M. F. P.: GLOBGM v1.0: a parallel implementation of a 30 arcsec PCR-GLOBWB-MODFLOW



- global-scale groundwater model, *Geosci. Model Dev.*, 17, 275-300, 10.5194/gmd-17-275-2024, 2024.
- 760 Wang, X., Tian, Y., Yu, J., Lancia, M., Chen, J., Xiao, K., Zheng, Y., Andrews, C. B., and Zheng, C.: Complex Effects of Tides on Coastal Groundwater Revealed by High-Resolution Integrated Flow Modeling, *Water Resour Res*, 59, e2022WR033942, <https://doi.org/10.1029/2022WR033942>, 2023.
- Wang, Y., Ma, R., Wang, W., and Su, X.: Preface: Groundwater sustainability in fast-developing China, *Hydrogeol J*, 26, 1295-1300, 10.1007/s10040-018-1820-4, 2018.
- 765 Westerhoff, R., White, P., and Miguez-Macho, G.: Application of an improved global-scale groundwater model for water table estimation across New Zealand, *Hydrol. Earth Syst. Sci.*, 22, 6449-6472, 10.5194/hess-22-6449-2018, 2018.
- Yamazaki, D., Ikeshima, D., Sosa, J., Bates, P. D., Allen, G. H., and Pavelsky, T. M.: MERIT Hydro: A High-Resolution Global Hydrography Map Based on Latest Topography Dataset, *Water Resour Res*, 55, 5053-5073, 10.1029/2019wr024873, 2019.
- 770 Yan, F., Shangguan, W., Zhang, J., and Hu, B.: Depth-to-bedrock map of China at a spatial resolution of 100 meters, *Sci Data*, 7, 2, 10.1038/s41597-019-0345-6, 2020.
- Yang, C., Tijerina-Kreuzer, D. T., Tran, H. V., Condon, L. E., and Maxwell, R. M.: A high-resolution, 3D groundwater-surface water simulation of the contiguous US: Advances in the integrated ParFlow CONUS 2.0 modeling platform, *J Hydrol*, 130294, <https://doi.org/10.1016/j.jhydrol.2023.130294>, 2023a.
- 775 Yang, C., Li, H.-Y., Fang, Y., Cui, C., Wang, T., Zheng, C., Leung, L. R., Maxwell, R. M., Zhang, Y.-K., and Yang, X.: Effects of Groundwater Pumping on Ground Surface Temperature: A Regional Modeling Study in the North China Plain, *Journal of Geophysical Research: Atmospheres*, 125, e2019JD031764, 10.1029/2019jd031764, 2020.
- 780 Yang, J. and Huang, X.: The 30th annual land cover dataset and its dynamics in China from 1990 to 2019, *Earth Syst. Sci. Data*, 13, 3907-3925, 10.5194/essd-13-3907-2021, 2021.
- Yang, Y., Feng, D., Beck, H. E., Hu, W., Sengupta, A., Monache, L. D., Hartman, R., Lin, P., Shen, C., and Pan, M.: Global Daily Discharge Estimation Based on Grid-Scale Long Short-Term Memory (LSTM) Model and River Routing, *ESS Open Archive*, DOI: 10.22541/essoar.169724927.73813721/v1, 2023b.
- 785 Yin, Z., Lin, P., Riggs, R., Allen, G. H., Lei, X., Zheng, Z., and Cai, S.: A synthesis of Global Streamflow Characteristics, Hydrometeorology, and Catchment Attributes (GSHA) for large sample river-centric studies, *Earth Syst. Sci. Data*, 16, 1559-1587, 10.5194/essd-16-1559-2024, 2024.
- 790 Yu, X., Luo, L., Hu, P., Tu, X., Chen, X., and Wei, J.: Impacts of sea-level rise on groundwater inundation and river floods under changing climate, *J Hydrol*, 614, 128554, <https://doi.org/10.1016/j.jhydrol.2022.128554>, 2022.
- Zhang, J., Condon, L. E., Tran, H., and Maxwell, R. M.: A national topographic dataset for hydrological modeling over the contiguous United States, *Earth Syst. Sci. Data*, 13, 3263-3279, 10.5194/essd-13-3263-2021, 2021.
- 795 Zhang, Y., Kong, D., Gan, R., Chiew, F. H. S., McVicar, T. R., Zhang, Q., and Yang, Y.: Coupled estimation of 500 m and 8-day resolution global evapotranspiration and gross primary



800 production in 2002–2017, *Remote Sens Environ*, 222, 165-182,
<https://doi.org/10.1016/j.rse.2018.12.031>, 2019.
Zhao, K., Fang, Z., Li, J., and He, C.: Spatial-temporal variations of groundwater storage in
China: A multiscale analysis based on GRACE data, *Resources, Conservation and
Recycling*, 197, 107088, <https://doi.org/10.1016/j.resconrec.2023.107088>, 2023.